Quantum-chemical study of organic reaction mechanisms. XI. *[1] The interaction of diformylhydrazine with *o*- and *p*-aminophenols producing biologically active 4-substituted 1,2,4-triazoles

E.A. Chirkina[a,b,*], L.I. Larina[a]

[a] *A.E. Favorsky Irkutsk Institute of Chemistry, Siberian Branch of the Russian Academy of Sciences, 1, Favorsky Str., 664033 Irkutsk, Russia*

[b] *Angarsk State Technical University, 60, Chaikovsky Str, 665835 Angarsk, Irkutsk region, Russia, e-mail: chirkina_ea@mail.ru*

A mechanism for the reaction of diformylhydrazine with o- and p-aminophenols has been studied by quantum-chemical calculations within the framework of electron density functional theory using the B3LYP/6-311++G (d,p)//B2PLYP/6-311++G (d, p) basis sets. It is shown that the first stage of this reaction involves nucleophilic addition of the aminophenol nitrogen to one of the carbonyl groups of diformylhydrazine to afford an unstable geminal amino alcohol, which can be further dehydrated to iminohydrazide or hydrazonamide. The prototropic imino-amine rearrangement occurring in the iminohydrazide delivers hydrazonamide, The latter, owing to nucleophilic attack of the nitrogen atom at the second carbonyl group, is converted into a cyclic amino alcohol, dehydration of which produces the target 1,2,4-triazole. The obtained results have been compared with the data NMR spectroscopy.

***Key words**: diformylhydrazine, o-, p-aminophenols, reaction mechanisms, nucleophilic addition, prototropic amino-imine rearrangement, electron density functional theory, B3LYP, potential energy surface, NMR spectroscopy.*

Introduction

Currently, special emphasis is given to the search for new biologically active substances to design efficient and harmless drugs. 1,2,4-Triazole structural motif is met in numerous medicines [2], which are efficient in the treatment of viral and fungal infections as well as cancer therapy. The derivatives of 1,2,4-triazole are known to exhibit antimicrobial, anticonvulsant, anti-inflammatory, immunomodulatory and other types of activity [3]. Some 1,2,4-triazoles are employed as pesticides and growth regulators [4]. They are also potential ligands for the synthesis of magnetoactive coordination compounds possessing optoelectronic, electrochemical, electrophysical and thermochemical properties [5-7]. 4-Substituted 1,2,4-triazoles exert radioprotective action [8]. Interest in this class of compounds is

[*] Previous publication X see [1]

* Corresponding author

constantly growing, which is evidenced from a large number of publications devoted to the chemical, biological, and structural features of 1,2,4-triazoles [9-12].

In continuation of our theoretical research on the mechanisms of organic reactions [1, 13], in this communication, we have studied the interaction of diformylhydrazine with aminophenols producing 4-substituted 1,2,4-triazoles.

Results and discussion

Earlier, [4] 4-substituted 1,2,4-triazoles were synthesized by fusion of diformylhydrazine with aminophenols at 145-170°C, the yields being 46% and 64% yields for the *ortho*- and *para*-isomers, respectively. The obtained 1,2,4-triazoles are stable crystalline substances with high melting points, soluble in ethanol and DMSO. The structure of the studied compounds was proved by multinuclear ^{1}H, ^{13}C, ^{15}N and two-dimensional NMR spectroscopy (COSY-gp, NOESY-gp, HSQC-gp, HMBC-gp) (Table).

The two-dimensional ^{15}N {^{1}H-^{15}N} HMBC NMR spectra of compounds (**3a**,**b**) show cross-peaks of nitrogen atoms with the triazole ring protons H-3,5 and the corresponding *ortho*-protons of the phenyl fragment at –59.9 ÷ –62.3 (N-1,2) ppm for the pyridine nitrogen, as well as in the range of –194.4 ÷ –211 (N-4) ppm for the pyrrole atom. This indicates that the heterocyclization occurs to deliver 1,2,4-triazoles.

Since the mechanism for the formation of 1,2,4-triazoles was not discussed in communication [4], the theoretical study of this reaction is of particular interest for understanding the heterocyclization process.

Table. ^{1}H, ^{13}C and ^{15}N NMR chemical shifts of 4-substituted 1,2,4-triazoles (3a, b) (DMSO-d_6, ppm)

N°	Compound	^{1}H	^{13}C	^{15}N		Yield %/ mp °C
				N-1,2	N-4	
3a	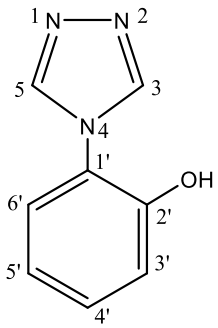	10.92 br s 1H OH 9.20 s 2H H-3,5 7.82 d 1H H-6’ $^{3}J_{HH}$ = 7.9 Hz 7.69 dd 1H H-4’ $^{3}J_{HH}$ = 8.2 Hz $^{3}J_{HH}$ = 8.0 Hz 7.48 d 1H H-3’ $^{3}J_{HH}$ = 8.2 Hz 7.33 dd 1H H-5’ $^{3}J_{HH}$ = 8.0 Hz $^{3}J_{HH}$ = 7.9 Hz	150.53 C 2’ 143.17 C 3,5 129.79 C 5’ 125.63 C 4’ 121.72 C 1’ 119.70 C 3’ 116.95 C 6’	-62.3	-203.4	46/ 214-216

3b	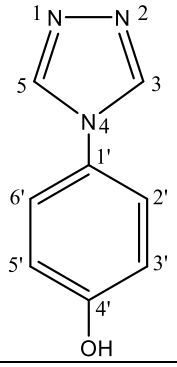	9.85 br s 1H OH 8.93 s 2H H-3,5 7.45 d 2H H-2'6' $^3J_{HH}$ = 8.7 Hz 6.90 d 2H H-3'5' $^3J_{HH}$ = 8.7 Hz	157.43 C 4' 141.82 C 3,5 125.85 C 1' 123.33 C2'6' 116.30 C3'5'	-59.9	-194.4	64/ 285-286

Therefore, in this work, we have studied the mechanism of the reaction of diformylhydrazine **1** with *o*-, *p*-aminophenols **2a**,**b** giving rise to 4-(*o*-, *p*-hydroxyphenyl)-1,2,4-triazoles **3a**,**b** [4] (Scheme 1) using quantum-chemical calculations.

Scheme 1

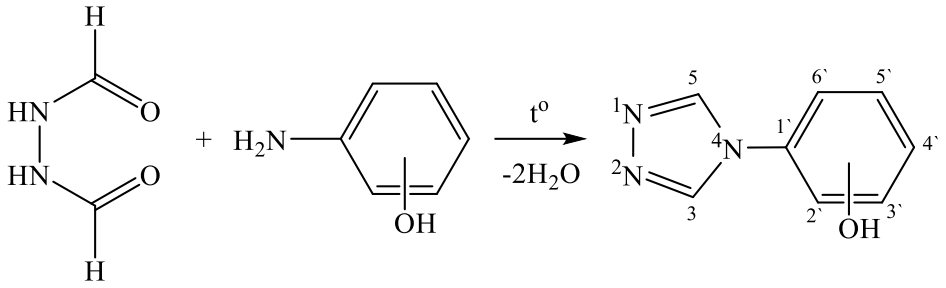

1 **2a**,**b** **3a**,**b**

Figure 1 shows the energy profiles of the above reaction. Free energies of reactants **1** and **2a**,**b** were taken as 0.0 kcal/mol.

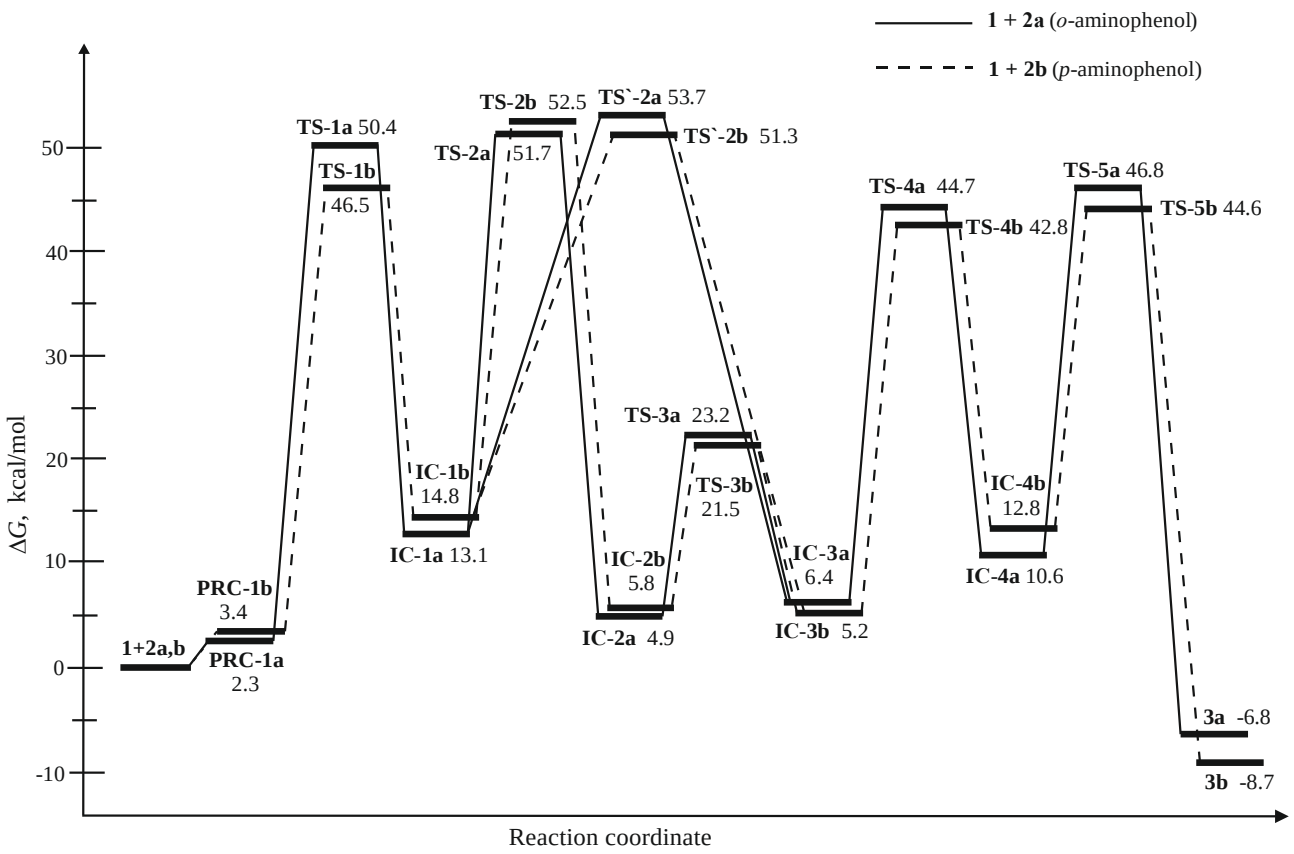

Figure 1. Energy profile of the interaction of diformylhydrazine (**1**) with *o*-, *p*-aminophenols (**2a**,**b**) giving 1,2,4-triazoles (**3a**,**b**). Relative free energies are given in kcal/mol.

Results of the calculations allow the following mechanism of the first stage of the reaction to be proposed (Scheme 2, Figure 2).

Scheme 2

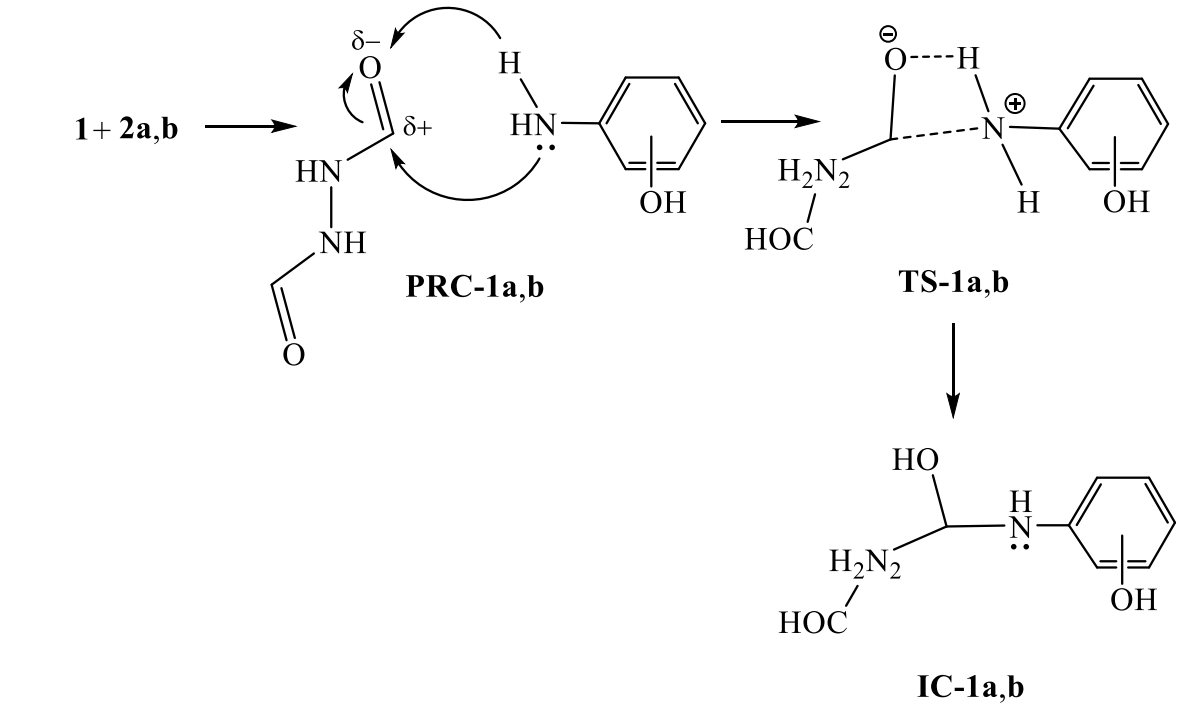

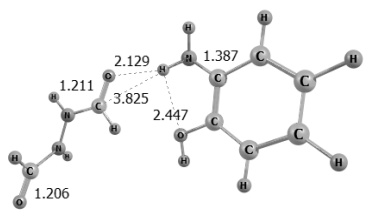

PRC-1a

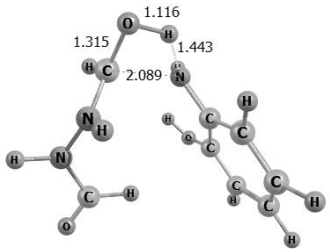

TS-1a (ν = -1295.3 cm^{-1})

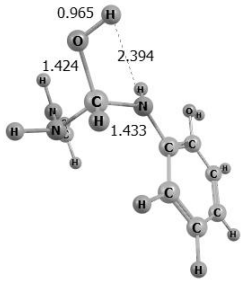

IC-1a

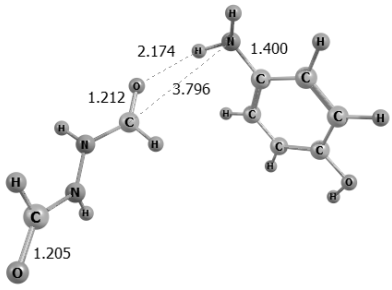

PRC-1b

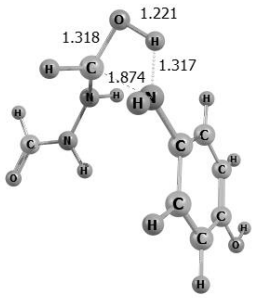

TS-1a (ν = -1757.2 cm^{-1})

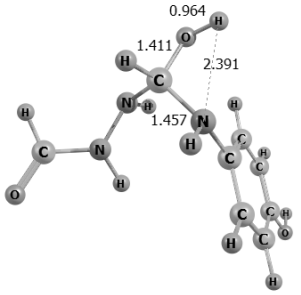

IC-1b

Figure 2. Spatial structure of pre-reaction complexes (**PRC-1a**,**b**), transition states (**TS-1a**,**b**) and intermediate compounds (**IC-1a**,**b**) optimized by the B3LYP/6-311++G (d,p). Bond lengths and interatomic distances are given in Å. The value of the imaginary vibrational frequency of the transition state, calculated from the Hessian matrix, is indicated in parentheses.

The first stage of the process involves localization of the pre-reaction complexes **PRC-1a**,**b**, the formation of which is accompanied by a slight increase in the free

energy of the system by 2.3 and 3.4 kcal/mol, respectively. **PRC-1a** complex is more stable (like *o*-aminophenol itself) due to the intramolecular hydrogen bond N–H… O–H.

In **PRC-1a,b** complexes, the amino function is almost opposite relative to a carbonyl group of diformylhydrazine, allowing the lone electron pair (LEP) of the nitrogen atom to be nucleophilically attacked at the electron-deficient carbon atom attack (Figure 2). The molecules of reactants in pre-reaction complexes undergo some geometric changes. Thus, in diformylhydrazine, the length of the C = O bond of a carbonyl group slightly increases by 0.006 Å and 0.009 Å, respectively; bond lengths in aminophenols C–NH_2 are also noticeably augmented, especially in **PRC-1a** (by 0.024 Å). As this reaction proceeds, the pre-reaction complexes **PRC-1a**,**b** are converted into intermediates **IC-1a**,**b** through four-center transition states **TS-1a**,**b** with activation barriers of $\Delta G^{\neq}$(**TS-1a**) = 48.1 kcal/mol and $\Delta G^{\neq}$(**TS-1b**) = 43.1 kcal/mol (Figure 1).

High energy barriers of the transformations of pre-reaction complexes into aminoalcohols are associated with the structural features of the reactants. For instanse, in aminophenol, a nitrogen electron pair is in *p*,*π*-conjugation with a phenyl group, which somewhat reduces its nucleophilicity. However, the presence of an electron-donating OH group in the benzene ring makes nitrogen LEP more susceptible to an electrophile. In diformylhydrazine, the positive charge on the carbonyl group carbon decreases due to electron-donating properties of the hydrazine moiety. These factors hinder the nucleophilic addition reactions A_N.

The localized transition states **TS-1a**,**b** are bipolar systems. The positive charge on the nitrogen atom is induced owing to its significant approach to the C=O group carbon (by 1.736 Å, 1.922 Å, respectively) and the formation of a covalent C-N bond with the participation of LEP. The addition of a nitrogen atom leads to a heterolytic cleavage of the π-bond, and a negative charge is located on the carbonyl oxygen atom, the bond between the carbon and oxygen atoms of the carbonyl group being noticeable increased by 1.105 Å. Also, one of the hydrogen atoms of the amino group approaches the carbonyl oxygen (by 1.013 Å, 0.953 Å, respectively) for further electrophilic attack. Next, the transition states are transformed into *α*-aminoalcohols **IC-1a**,**b** that reduces free energy of the system by more than 30 kcal/mol (Fig. 1).

Geminal amino alcohols **IC-1a**,**b** are unstable and can further eliminate water. It can be assumed that the intramolecular dehydration can proceed in two directions to afford: (*I)* iminohydrazides **IC-2a**,**b**, when, together with the elimination of the OH group, NH hydrogen of the aminophenol fragment is cleaved; (*II)*

hydrazonamides **IC-3a**,**b**, when NH hydrogen of the hydrazine moiety participates in dehydration (Scheme 3, Figure 3).

Scheme 3

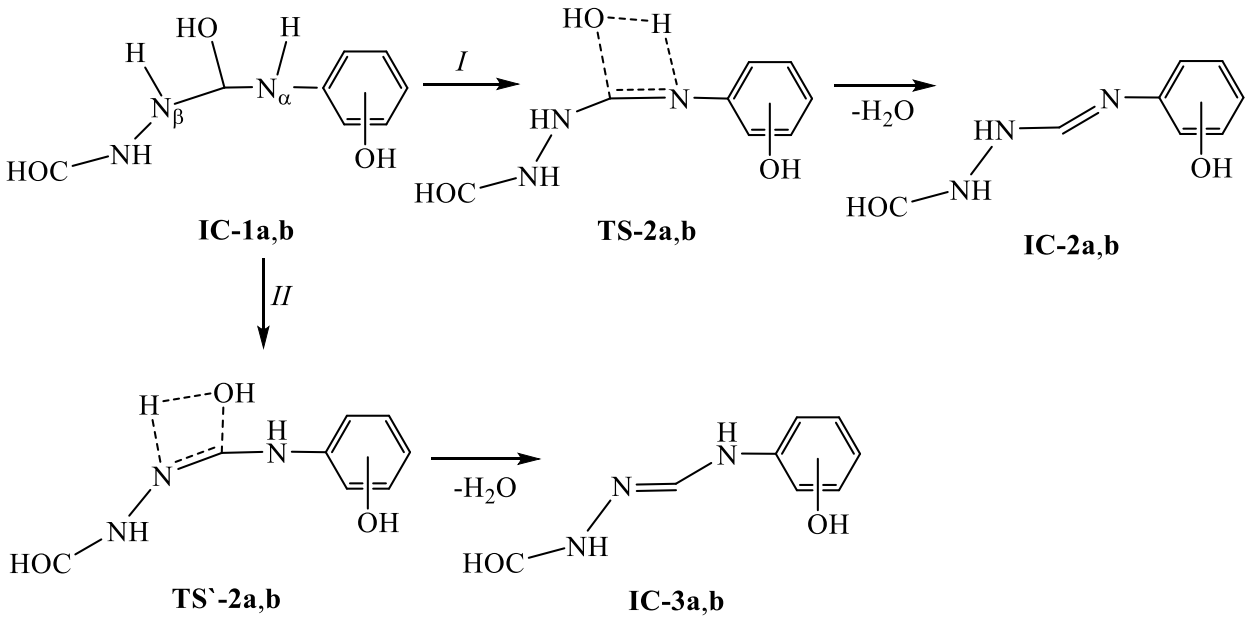

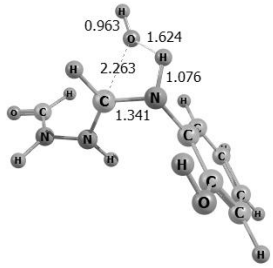

TS-2a (ν = -439.3 cm^{-1})

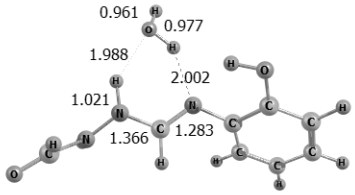

IC-2a

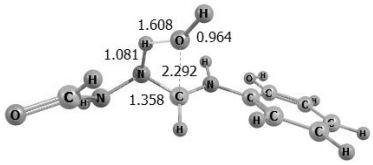

TS`-2a (ν = -507.0 cm^{-1})

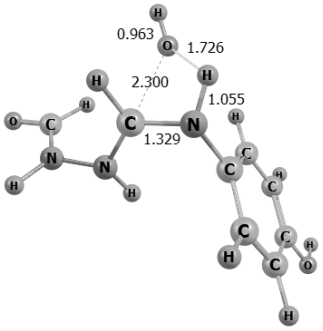

TS-2b (ν =-318.3 cm^{-1})

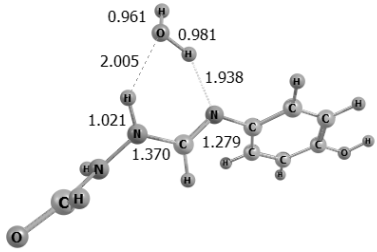

IC-2b

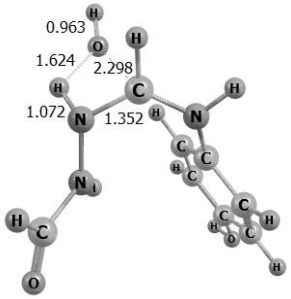

TS`-2b (ν = -370.1 cm^{-1})

Figure 3. Spatial structure of transition states (**TS-2a**,**b**; **TS`-2a**,**b**) and intermediate compounds (**IC-2a**,**b**) optimized by the B3LYP/6-311++G (d,p) method. Bond lengths and interatomic distances are given in Å. The value of the imaginary vibrational frequency of the transition state, calculated from the Hessian matrix, is indicated in parentheses.

The first direction is implemented through the four-center transition states TS-**2a**,**b** with activation barriers of $\Delta G^{\neq}$(**TS-2a**) = 38.6 kcal/mol and $\Delta G^{\neq}$(**TS-2b**) = 37.7 kcal/mol. In this case, a significant increase in the lengths of the C-O bonds by 0.839 Å (0.889 Å) and N_{α}-H bonds by 0.063 Å (0.045 Å) is observed. The C-N_{α} bond, on the contrary, is shortened by 0.092 Å (0.128 Å), and becomes a double bond (here and below, the geometric parameters for the reaction system with the participation of *p*-aminophenol are given in parentheses).

The second direction involves the formation of four-center transition states **TS`-2a**,**b** with activation barriers of $\Delta G^{\neq}$(**TS`-2a**) = 40.7 kcal/mol and $\Delta G^{\neq}$(**TS`-2b**) = 36.5 kcal/mol. In this case, the lengths of the C-O and N_{β}-H bonds also significantly increase by 0.873 Å (0.887 Å) and 0.056 Å (0.057 Å), while the C-N_{β} bond is shortened by 0.103 Å (0.109 Å) (Fig. 3).

The comparison of the activation barriers for **TS-2a**,**b** and **TS`-2a**,**b** shows that for the *o*-aminophenol derivative, the first direction of dehydration is accompanied by a lower energy barrier to produce more stable state **IC-2a**. In case of *p*-aminophenol derivative, on the contrary, the second direction of dehydration proceeds more easily to furnish a more stable intermediate **IC-3b** (Figure 1).

Iminohydrazides **IC-2a**,**b** and hydrazonamides **IC-3a**,**b**, formed via elimination of water, are thermodynamically stable systems due to the *p*,*π*-conjugation of *α*-nitrogen LEP with π-system of the benzene ring, and in the intermediates **IC-3a**,**b** also with the C=N_{β} bond It should be noted that possible *π*,*π*-conjugation in the intermediates **IC-2a**,**b** is hindered by the spatial arrangement of the C=N_{α} bond, which deviates from the conjugation plane of the aromatic system by more than 40°. Interestingly, that during the formation of iminohydrazides and hydrazonamides, free energy of the system decreases by approximately 47 kcal/mol (Figure 1).

If direction *I* is implemented, the imino-amine tautomerism can occur in iminohydrazides **IC-2a**,**b** to increase nucleophilicity of the imine nitrogen, which further attacks the carbon atom of the second carbonyl group. The migration of a proton from the NH group of the hydrazine fragment to the imine nitrogen involves direct participation of a water molecule, which is present in each reaction system after dehydration of *α*-amino alcohols **IC-1a**,**b** (Scheme 4).

Scheme 4

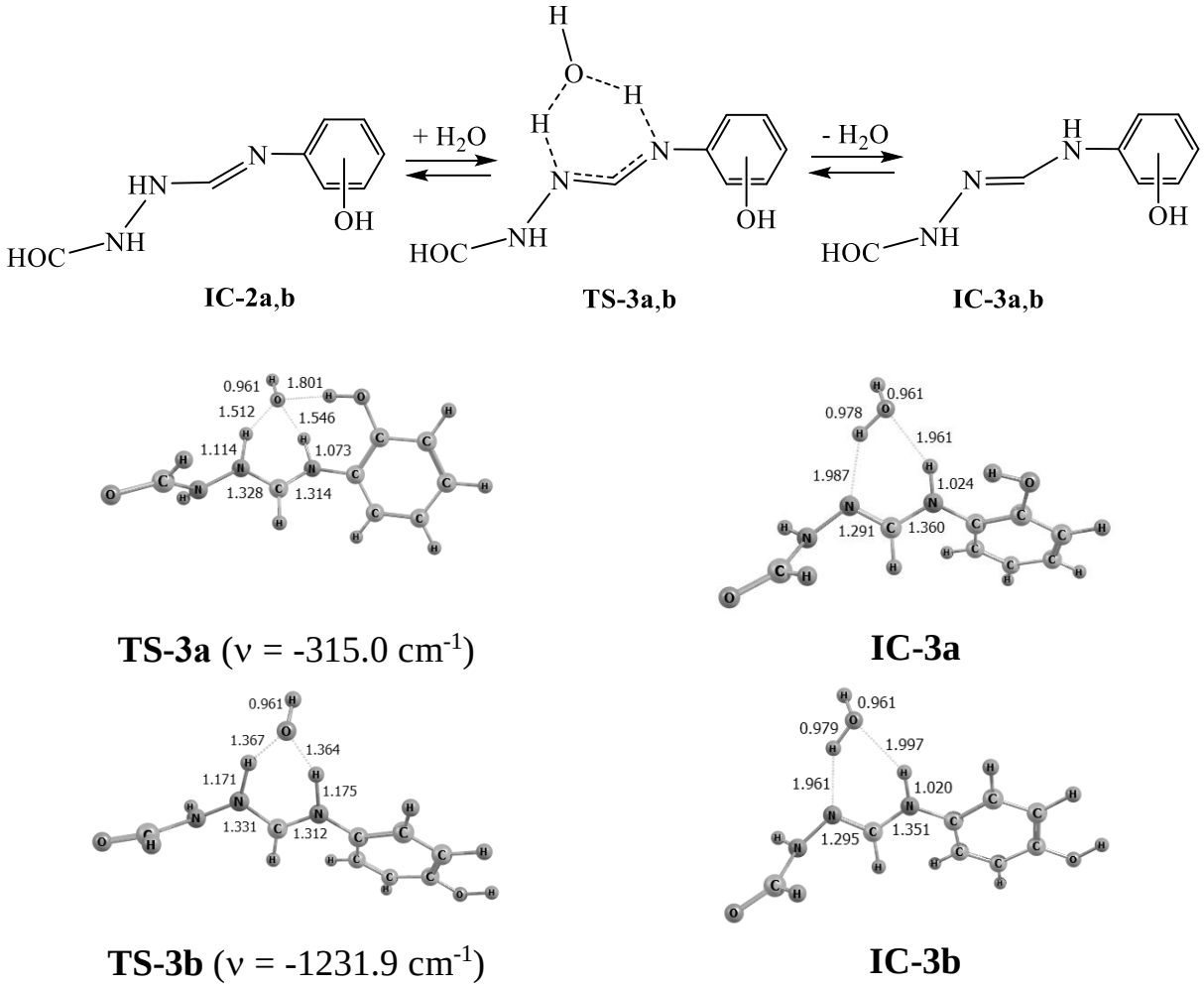

Figure 4. Spatial structure of transition states (**TS-3a**,**b**) and intermediate compounds (**IC-3a**,**b**) optimized by the B3LYP/6-311++G (d,p) method. Bond lengths and interatomic distances are given in Å. The value of the imaginary vibrational frequency of the transition state, calculated from the Hessian matrix, is indicated in parentheses.

Intermediates **IC-2a**,**b** rearrange into **IC-3a**,**b** via six-center transition states **TS-3a**,**b** with activation barriers of $\Delta G^{\neq}$(**TS-3a**) = 18.3 kcal/mol and $\Delta G^{\neq}$(**TS-3b**) = 15.7 kcal/mol.

An analysis of the geometric parameters of the transition states **TS-3a**,**b** reveals that the water molecule, on the one hand, provides the imine nitrogen with one of its hydrogen atoms, while the O-H bond significantly increases by 0.569 Å (0.383 Å), and the distance N… H-OH is significantly reduced by 0.929 Å (0.763 Å). On the other hand, the water molecule pulls away hydrogen from the hydrazine nitrogen, while the N-H bond increases by 0.093 Å (0.150 Å), and the H-O… H-N distance decreases by 0.476 Å (0.638 Å). The proton transfer is accompanied by the migration of the C=N bond.

If direction *II* is realized, the intermediates **IC-3a**,**b** can be directly obtained avoiding the stage of imine-amine rearrangement (Scheme 3).

In each of the formed intermediates **IC-3a**,**b**, LEP of the aminophenol nitrogen affects the electron-deficient carbonyl carbon to afford cyclic *α*-amino alcohols **IC-4a**,**b**, while the free energy of the system decreases by 30 kcal/mol (Scheme 5).

Scheme 5

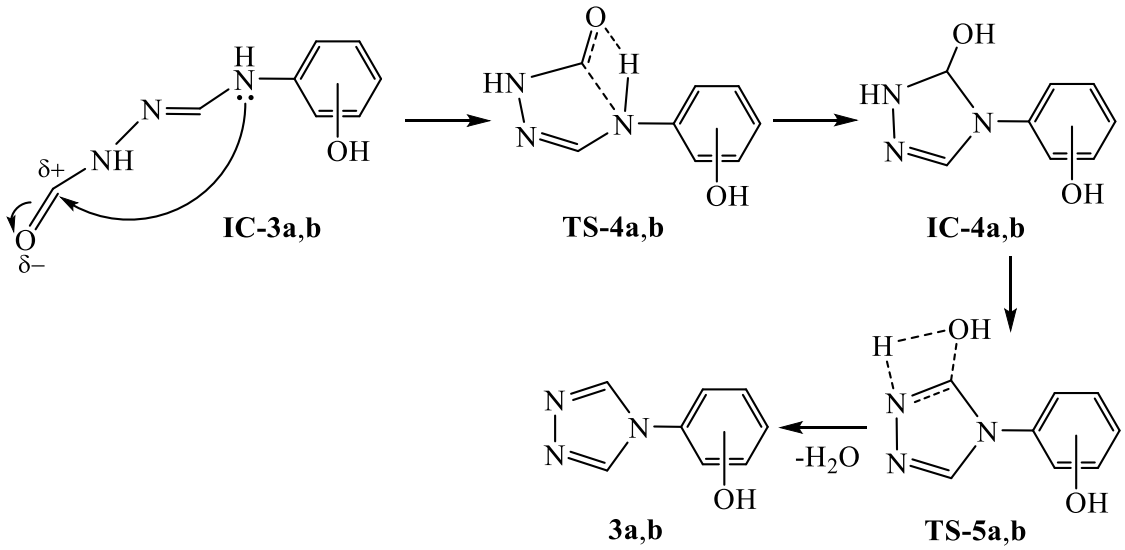

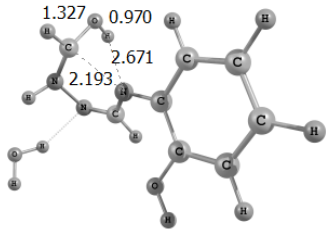

TS-4 a (-280.2)

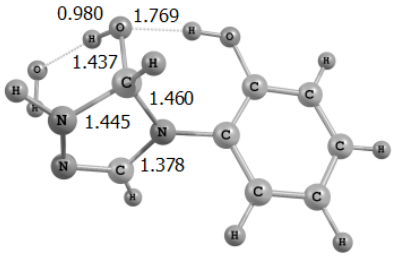

IC-4 a

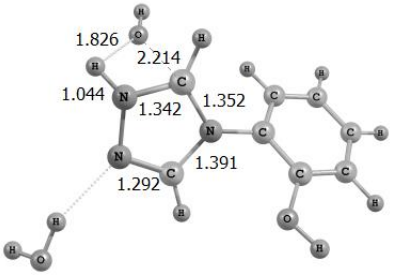

TS-5 a (-331.5)

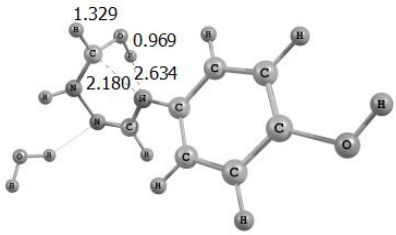

TS-4 b (-292.2)

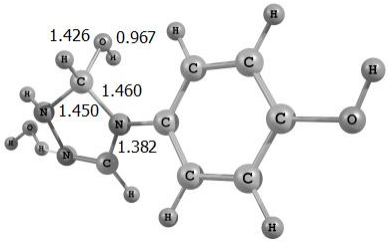

IC-4 b

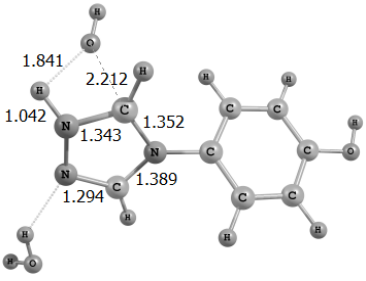

TS-5 b (-322.0)

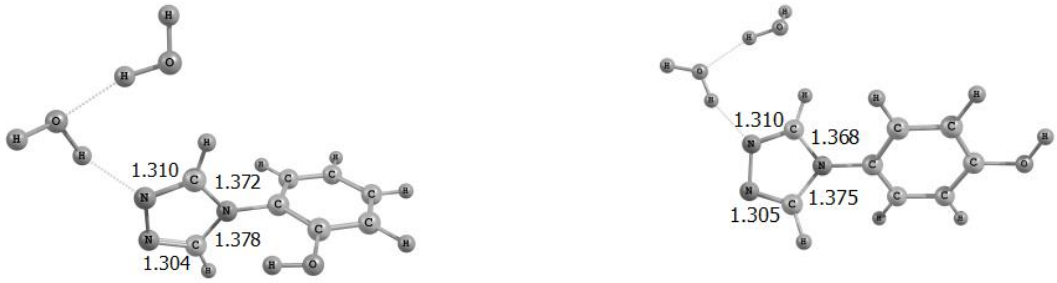

3a **3 b**

Figure 5. Spatial structure of transition states (**TS-4a**,**b**; **TS-5a**,**b**), intermediate compounds (**IC-4a**,**b**) and reaction products (**3a**,**b**) optimized by the B3LYP/6-311++G (d,p). Bond lengths and interatomic distances are given in Å. The value of the imaginary vibrational frequency of the transition state, calculated from the Hessian matrix, is indicated in parentheses.

The heterocyclization proceeds through the transition states **TS-4a**,**b** with significant activation barriers of $\Delta G^{\neq}$(**TS-4a**) = 38.3 kcal/mol and $\Delta G^{\neq}$(**TS-4b**) = 37.6 kcal/mol (Fig. 4).

In the transition states **TS-4a**,**b**, the diformylhydrazine carbonyl group is turned to the attacking nitrogen atom, which enlarges the C-N-N-C torsion angle by 26.2° (33.3°), while the N ... C distance significantly decreases by 2.041 Å (2.062 Å) and the C=O bond lengs increases by 0.108 Å (0.116 Å) (Fig. 5). Afterwards, the transition states are transformed into cyclic *α*-aminoalcohols **IC-1a**,**b** with reduction free energy of the system by more than 30 kcal/mol (Fig. 1).

Further, intramolecular dehydration of cyclic α-amino alcohols **IC-4a**,**b** proceeds through four-center transition states **TS-5a**,**b** with activation barriers of $\Delta G^{\neq}$ (**TS-5a**) = 36.2 kcal/mol and $\Delta G^{\neq}$(**TS-5b**) = 31.8 kcal/mol (Fig. 1). In this case, the length of the C-O bonds is augmented by 0.777 Å (0.786 Å), while the N-H bonds slightly increase by 0.032 Å (0.028 Å). The C-N bond, on the contrary, becomes shorter by 0.103 Å (0.107 Å) and becomes unsaturated (Fig. 5).

The formation of the target products, 4-(*o*-,*p*-hydroxyphenyl) -1,2,4-triazoles **3a**,**b**, diminishes free energy of the system by more than 50 kcal/mol. Analysis of the geometric parameters of 4-(*o*-hydroxyphenyl)-1,2,4-triazole evidences the presence of a weak intramolecular hydrogen bond between the hydroxy group of the phenol fragment and the C–H bond of the triazole ring C–H… O–H (2.618 Å). Indeed, the experimental NMR data indicate the hydrogen bonding in the *ortho*-hydroxyphenyl derivative of 1,2,4-triazole (**3a**) (Table). In the ^{1}H NMR spectra of compound **3a**, a downfield shift of the broadened OH signal by more than 1 ppm is observed compared to the *para*-derivative. The position of the OH group in the phenyl fragment slightly effects on the values of the ^{1}H and ^{13}C chemical shifts.

Conclusion

In conclusion, the calculations have shown that the first stage of the studied reaction involves nucleophilic addition of *ortho*- or *para*-aminophenol at a carbonyl group of diformylhydrazine to deliver unstable α-amino alcohol followed by its dehydration. The dehydration of *p*-aminophenol-derived α-amino alcohol can immediately afford an intermediate product, hydrazonamide. If α-amino alcohol is formed from *o*-aminophenol, its dehydration can give rise to iminohydrazide, which is further transformed into hydrazonamide due to prototropic imino-amine rearrangement. The next stage of the studied interaction is the heterocyclization of hydrazonamide via a nucleophilic attack of the nitrogen atom at the second carbonyl group to furnish a cyclic α-amino alcohol, which, after the elimination of water, is converted into the target 1,2,4-triazole.

Experimental

The ^{1}H, ^{13}C and ^{15}N NMR spectra were recorded in DMSO-d_6 solutions at room temperature on Bruker DPX-400 and AV-400 spectrometers (400.13, 100.61 and 40.56 MHz, respectively). ^{1}H, ^{13}C and ^{15}N Chemical shift values (δ in ppm) were measured with accuracy of 0.01, 0.02 and 0.1 ppm, respectively, and referred to TMS (^{1}H, ^{13}C) and nitromethane (^{15}N). The assignment of ^{1}H and ^{13}C signals in spectra was performed using 2D heteronuclear correlation HMBC-gp and HSQC-gp ^{13}C-^{1}H methods. The values of the δ^{15}N were obtained through the 2D ^{1}H-^{15}N HMBC-gp experiment. Coupling constants (*J* in Hz) values approaches to 0.1 Hz.

Preliminary optimization of the geometric parameters of all reaction participants was carried out in the PRIRODA 6.0 software package by the DFT–PBE /3ζ method [14]. The final optimization of the geometry of all localized stationary points, the search for transition states, and harmonic vibrational analysis were performed using the GAUSSIAN 09 software package [15] within the framework of the electron density functional theory by the B3LYP/6-311++G (d, p) method. The energies of stationary points were refined using a one-point calculation using the B2PLYP/6-311++G (d, p) method.

The search for transition states was carried out by the method of relaxed scanning along the reaction coordinate, and the localization of the structures of the transition state was performed according to the Bernie algorithm [16]. To prove that the obtained transition states correspond to the directions of this interaction, we used the procedure of following along the internal coordinate of the reaction by the Gonzalez-Schlegel method [17, 18].

Since this reaction was experimentally carried out by fusing the reagents without using a solvent, the calculation of the studied interaction was carried out in the gas phase.

Research Resources

Optimization of geometric parameters and calculation of molecular properties were performed by the B3LYP/6-311++G (d,p) method using the GAUSSIAN 09 program [16] at A.E. Favorsky Irkutsk Institute of Chemistry SB RAS on the computing cluster of the Baikal Analytical Center for Collective Use of the SB RAS (http://ckp-rf.ru/ckp/3050/). Experimental NMR results were also obtained with use of the equipment of the Baikal Analytical Centre for Collective Use of the SB RAS.

Conflict of interests

The authors declare that they have no conflicts of interest.

References

[1] E. A. Chirkina, L. B. Krivdin, B. C. Nikonova, V. A. Grabel′nyh, N. A. Korchevin, I. B. Rosentsveig, *Russ. J. Org. Chem.* **2021**, 57, 1073.

[2] D. Richards, J. Coleman, J. Reynolds, J. Aronson, Oxford Handbook of Practical Drug Therapy. Oxford; New York: Oxford University Press, **2011**.

[3] R. D. Porsolt, M. L. Pichon, M. Jalfre, *Nature*. **1977**, *266*, 730.

[4] V. N. Elokhina, A. S. Nakhmanovich, T. I. Yaroshenko, Z. V. Stepanova, L. I. Larina, *Russ. J. Gen. Chem.* **2006**, *76*, 161.

[5] J. G. Haasnoot, *Coord. Chem. Rev*. **2000**, *200-202*, 131.

[6] G. Aromí, L. A. Barrios, O. Roubeau, P. Gamez, *Coord. Chem. Rev.* **2011**, *255*, 485

[7] E. V. Lider, E. B. Peresypkina, K. G. Lavrenova, L. A. Sheludyakova, A. I. Smolentsev, T. I. Yaroshenko, V. N. Elokhina, *Coord. Chem.* **2012**, *38*, 367.

[8] V. G. Yashunskii, *Russ. Chem. Review.* **1975**, *44*, 531.

[9] B. Modzelewska-Banachiewicz, A. Chodkowska, E. Jagiełło-Wójtowicz, L. Mazur, *Eur. J. Med. Chem*. **2004**, *39*, 873.

[10] A. P. Engoyan, V. A. Pivazyan, E. A. Kazaryan, R. S. Akopyan, *Russ. J. Gen. Chem.* **2019**, *89*, 37.

[11] L. I. Larina, V. A. Lopyrev, Nitroazoles: Synthesis, Structure and Application. Springer. New York. **2009**. 446 p.

[12] L. I. Larina, Tautomerism and Structure of Azoles: Nuclear Magnetic Resonance Spectroscopy. *Adv. Heterocyc. Chem.* **2017**, *124*, 233-321.

[13] E. A. Chirkina, L. I. Larina, T. N. Komarova, *J. Organometal. Chem*. **2020**, *915*, 1.

[14] D. N. Laikov, Yu. A. Ustynyuk, *Russ. Chem. Bull., Int. Ed*., **2005**, *54*, 820.

[15] Gaussian 09, Revision C.01, M. J. Frisch, G. W. Trucks, H. B. Schlegel, G. E. Scuseria, M. A. Robb, J. R. Cheeseman, G. Scalmani, V. Barone, B. Mennucci, G. A. Petersson, H. Nakatsuji, M. Caricato, X. Li, H.P. Hratchian, A.F. Izmaylov, J. Bloino, G. Zheng, J.L. Sonnenberg, M. Hada, M. Ehara, K. Toyota, R. Fukuda, J. Hasegawa, M. Ishida, T. Nakajima, Y. Honda, O. Kitao, H. Nakai, T. Vreven, J. A. Montgomery, J. E. Peralta, F. Ogliaro, M. Bearpark, J.J. Heyd, E. Brothers, K.N. Kudin, V.N. Staroverov, R. Kobayashi, J. Normand, K. Raghavachari, A. Rendell, J.C. Burant, S.S. Iyengar, J. Tomasi, M. Cossi, N. Rega, J.M. Millam, M. Klene, J.E. Knox, J.B. Cross, V. Bakken, C. Adamo, J. Jaramillo, R. Gomperts, R.E. Stratmann, O. Yazyev, A.J. Austin, R. Cammi, C. Pomelli, J.W. Ochterski, R.L. Martin, K. Morokuma, V.G. Zakrzewski, G.A. Voth, P. Salvador, J.J. Dannenberg, S. Dapprich, A.D. Daniels, Ö. Farkas, J.B. Foresman, J.V. Ortiz, J. Cioslowski, and D.J. Fox, Gaussian, Inc., Wallingford CT, **2009**.

[16] B. J. Berne, M. Tuckerman, G. J. Martyna, *Chem. Phys*. **1991**, *94*, 6811.

[17] C. González, H. B. Schlegel, *J. Phys. Chem*. **1990**, *94*, 5523.

[18] C. González, H. B. Schlegel, *J. Chem. Phys*. **1991**, *95*, 5853.